Flexibility of Controllable Power Transformers for Managing Wind Uncertainty using Robust Adjustable Linearized Optimal Power Flow

Ahmad Nikoobakht[1], Jamshid Aghaei[2,3], Hossein Farahmand[3], Venkatachalam Lakshmanan[3], and Magnus Korpås[3]

[1] Department of Electrical Engineering, Higher Education Center of Eghlid, Eghlid, Iran (email: a.nikoobakht@eghlid.ac.ir)
[2]Department of Electrical and Electronics Engineering, Shiraz University-of-Technology, Shiraz, Iran,- (e-mails: aghaei@sutech.ac.ir)
[3]Department of Electric Power Engineering, Norwegian University of Science and Technology (NTNU), Trondheim NO-7491, Norway (hossein.farahmand@ntnu.no , vela@ntnu.no, magnus.korpas@ntnu.no)

[*]*Corresponding Author*: A. Nikoobakht, a.nikoobakht@eghlid.ac.ir

Abstract: **As renewable energy sources (RESs) penetration increases in the power system, the transmission system operators (TSOs) face new challenges to ensure system reliability and flexibility while ensuring high utilization of uncertain RES generation. Controllable transformers with on-load tap changers and phase sifting capability are the promising flexibility tools to keep the system acceptable security and flexibility levels by controlling the voltage levels and energy flow. The AC optimal power flow (AC OPF) with detailed modeling considerations such as the bus voltage magnitude by including these devices is challenging. This paper develops the AC OPF model to propose a robust flexibility optimization framework for daily scheduling problem with uncertain wind energy sources. Nevertheless, the proposed formulation representation is an intractable mixed integer nonlinear programming (MINLP) while it includs AC grid constraints and the augmented modeling of the mentioned transformers. Accordingly, the proposed MINLP problem has been converted into a mixed-integer linear program (MILP) where a certain level of solution accuracy can be achieved for the available time budget. The effectiveness of the proposed method is demonstrated using a modified six-bus and IEEE 118-bus test systems.**

Index Terms—wind power generation, controllable power transformers, optimal power flow, robust optimization.

Nomenclature

1) Indices:

g Index for thermal unit.
w Index for wind farm.
n, m Indices of buses.
k Index of lines.
t, t' Indices of time.

3) Continuous Variables:

$\delta_{nm}^{(\cdot)}$ Phase angle difference across line (n, m) at time t.

φ_k Phase of the phase shifting transformer k.

T_k Tap ratio of tap changing transformer k.

$V_{nt}^{(\cdot)}$ Voltage magnitude at bus n at period t.

$P_{gt}^{(\cdot)}$ / $Q_{gt}^{(\cdot)}$ Active/ reactive power generation of unit g at period t.

P_{wt}^{b} Dispatch of wind farm w at time t in the base case.

P_{wt}^{u} Adaptive generation change of wind unit w at time t as a reaction to uncertainty.

$P_{f,wt}^{u}$ Uncertain generation of wind farm w at time t.

PL_t Powre loss at period t.

fl_{nmkt}^{P} / fl_{nmkt}^{q} Active/reactive power flow on line k (n, m).

$\Psi_{(\cdot)}, \Upsilon_{(\cdot)}$ Slack variables.

$\Re_t$ / $\Im$ Mismatch of base case/worst case realizations sub-problems.

$\kappa_{(\cdot)}$ Dual variable of constraint.

$\xi_{(\cdot)}^{(\cdot)}$ / $\varsigma_{(\cdot)}^{(\cdot)}$ Dual variables.

4) Binary Variables:

v_{gt} / w_{gt} Startup/ shutdown variable for unit g and period t (1 for startup/ shutdown, 0 otherwise).

u_{gt} Status of unit g at period t

5) Constants:

$\tilde{P}_{wt}$ Generation deviation of wind farm w from the forecast value at time t.

D_{nt} / Q_{nt} Active/reactive power load.

$\Delta\Phi_g$ Up/down corrective action limit of unit g.

g_k / b_k Conductance of line k, a non-negative value.

C_g^b Cost of normal condition of thermal unit g.

C_{gt}^{SU} / C_{gt}^{SD} Startup (SU)/shutdown (SD) cost of thermal unit g at time t.

$P_g^{\max}$ / $P_g^{\min}$ Max/min active power generation.

$q_g^{\max} / q_g^{\min}$ Max/min reactive power generation.
R_g^{SU} / R_g^{SD} Max start-up/shutdown ramp rate for unit *g*.
R_g^{+} / R_g^{-} Max ramp up/ramp down rate for unit *g*.
γ_{dt} Power factor for reactive power load *d*.
$V_n^{\max} / V_n^{\min}$ Max/min of voltage magnitude.
$\delta_k^{\max} / \delta_k^{\min}$ Max/min of angle difference across line *k*.
$\varphi_k^{\max} / \varphi_k^{\min}$ Max/min phase of the PHS transformer *k*.
$L_k^{\max} / \tilde{L}_k^{\max}$ Max limit for active/reactive power flow of line *k*.
UT_g / DT_g Min ON/OFF time limit of unit *g*.
$\alpha_{nm\_\ell} / \beta_{nm\_\ell}$ lope of the ℓ *th* piecewise linear block/ value of the linearized $\cos(\delta_{mn})$ at ℓ *th* piecewise linear block

6) Abbreviations

OPF	Optimal power flow.
WPG	Wind power generation.
CPT	Controllable power transformer.
DC	Direct current.
AC	Alternative current.
TCT	Tap changing transformer.
PST	Phase shifting transformer.
SA	Stochastic approach.
RA	Robust approach.
MINLP	Non-convex mixed integer nonlinear programming.
NLP	Non-linear problem.
MILP	Mixed integer linear program.
PWL	Piece wise linearization.
LAC-RDAS	Linearized AC robust daily scheduling.
CCOTU	Corrective capacity of thermal unit.
OC	Operation cost.
MP	Master problem.
UC	Unit commitment.
VM	Voltage Magnitude.

1. Introduction

Nowadays, renewable energy generations are increasing significantly, among which wind power generation (WPG) takes a large portion [1]. Nevertheless, the increasing penetration of intermittent WPG, it introduces uncertainties to daily scheduling problem. The managing of WPG uncertainty is difficult, as the power grid is considered for conventional dispatchable thermal units rather than intermittent renewable generations. A trivial but unappealing to solve this problem would be to construct new transmission lines. But, constructing new transmission lines are enormously expensive, take numerous years to complete, and are not favored via the people living near the new lines. An environmentally, cheaper, and faster more appealing alternative to constructing new transmission lines is more effective utilization of the existing transmission grid and harness the flexibilities of the transmission grid, before constructing new transmission lines. This objective can be attained with controllable power transformers (CPTs), including tap changing transformers (TCTs) [2-5] and phase shifting transformers (PSTs) [2, 3, 6-8]. In recent years, these CPTs have been invented and increasingly deployed to control a number of power system parameters, such as voltage magnitude and phase [2, 3]. The CPTs can control line flows and help to reduce line flow on fully loaded transmission branches, which would lead to enhanced load handling capacity of the power system, improved power system security and flexibility, and eventually a further energy efficient transmission grid [2, 3, 6]. The ability to control line flows, will become more crucial as the share of WPG uncertainty increases in the power system operation [2]. This is because of the fact that the uncertainty of WPG will lead to unique transmission congestion patterns with rates never seen before. Generally the CPTs application problems (with renewable resources) is a large-scale and complex optimization problem and extremely challenging to solve they within a reasonable time with existing computational power, so, to overcome with these challenges, some of the previous research works have neglected the uncertainty sources (i.e., load or/and renewable uncertainty sources) and developed deterministic models [3, 4, 6-8], and also, some of these research works have considered DC power flow equations instead of AC ones [6, 7]. For example, in [6], an optimal power flow (OPF) problem with PST application has been studied but any uncertainty sources have not been considered. Similarly, in Ref [8] presents an OPF problem with PST application which maximize the utilization of WPG while decreasing transmission congestion. However, the OPF model in this research work is a deterministic model and wind uncertainty has been ignored. On the other hand, in Ref [6], the effect of optimal sitting of PST on minimize total generation cost in deterministic OPF problems has been considered, but in this research, the PST application modeled based on DC model and also uncertainty resources has been neglected. In Ref [4] the influence of TCT in a power system to regulator voltage profile as well as the distribution of power flow has been investigated, but wind uncertainty have not been considered by this research work. Finally, with neglecting the uncertainty sources and AC power flow equations more challenges emerge in daily scheduling problem. Accordingly, once uncertainty sources neglecting the daily scheduling problem become a deterministic problem, so, a deterministic daily scheduling problem needs to involve corrective capacities of online conventional thgermal units, but these capacities are decided by ignoring the uncertainty sources, and may lead to either insecure or high operation costs. Therefore, a suitable modeling of WEG uncertainty in daily scheduling formulation is highly required. The available uncertainty models in daily scheduling problems are categorized in two classifications:

Stochastic approach (*SA*): The SA has been extensively use [9, 10], it describes the uncertain parameters by means of scenarios. Therefore, the optimal solution of daily scheduling problem with SA is only guaranteed to be feasible for the scenarios considered in the problem. Additionally, the

complex optimization of a SA problem depends on the number of scenarios and number of uncertain parameters. Hence, the daily scheduling problem with SA faces two major challenges:

(i)- The SA requires large number of scenarios to model the uncertain parameter which results in high computational burden.

(ii)- The optimal solution of daily scheduling problem with SA is dependent on the accuracy of statistical data, statistical data with high accuracy is rarely available in practice.

Robust approach (*RA*): To overcome SA difficulties, the RA has newly engrossed an increasing attention [9, 11]. With respect to SA, this one does not rely on the number of scenarios, instead, it considers bounded intervals for the uncertain parameters [9]. Also, the RA only considers the worst case scenario of the system realizations to have a more computationally efficient approach [11]. Furthermore, the RA can adjust the solution conservativeness with the parameter called robustness degree. Nevertheless, most of the available literature applies the RA on the DC model rather than AC one to model the daily scheduling problems with wind and load uncertainty models [11-15]. But, the RA based on DC power flow equations is undesirable for the following reasons. First, in the RA based on DC model, reactive powers and voltage magnitudes as well as their constraints are neglected. As a result, the obtained solutions might be inaccurate or even insecure. Second, the RA based on DC model is unsatisfactory as the DC model's solutions cannot guarantee AC feasibility and the system security might be jeopardized once the CPTs (i.e., TCT and PST) are employed. Third, the DC model cannot be employed to benefit from other potential capabilities of the TCT and PST involvement in system operation, such as voltage support and congestion management. Also, in Refs [6, 7], the PST application has been modeled by DC model, as a result, the obtained solutions might be inaccurate or even insecure. To overcome these drawbacks, the AC network security constraints modeling is used to apply RA theory in this paper. However, implementing AC model in robust daily scheduling problem with CPTs yields a non-convex mixed integer nonlinear programming (MINLP) problem since it includes both integer variables and nonlinear of AC power flow equations as well as the TCT and PST models. Accordingly, resulting MINLP model is intractable to be solved by traditional MINLP solvers [10, 16]. Consequently, the robust daily scheduling problem with CPTs based on the AC model may not be a tractable problem even for small size systems which boosts research on to develop an efficient tractable model for it. Dealing with this issue, in some papers, the newton–raphson method has been used [17]; however, this method depends on the starting values and cannot easily handle inequalities. However, many heuristic methods, such as genetic algorithm [18], particle swarm optimization [18] were successfully applied to the power flow problem involving TCT and PST. However, these heuristic methods do not guarantee the global optimum solution.

On the other hand, in [3] provides an OPF-based security-driven re-dispatching procedure to assist the system operator to ensure an appropriate level of security with FACTS devices, i.e., the TCT and PST. In this Reference, the OPF formulation with TCT and PST models has been modeled by AC model, but, in OPF formulation, proposed in this reference, binary variables have not been considered, for this reason, this problem is only a non-linear problem (NLP). It should be noted that available solvers for NLP problems, in particular CONOPT and COUENNE, perform well to solve the proposed problem, in terms of convergence characteristics and computational time [19, 20]. Not that, the CONOPT and COUENNE are name two well-known solvers. But these solvers do not perform well to solve our proposed problem, i.e. MINLP and the solution might not be a global one [10, 21]. Consequently there are not effective solution methods to solve our proposed problem, in particular when the power system is of large-scale [10]. Therefore, it creates interest to develop tractable robust daily scheduling problem with AC security constraints. To overcome the challenges discussed above, the linearized AC power flow equations consider reactive power and voltage magnitude and also based on linearization process linear TCT and PST models have been proposed in this work, so, the proposed linearization process convert MINLP problem into a mixed integer linear program (MILP) without loss of the model accuracy which is also compatible with existing market solvers. On the other hand, solve a robust daily scheduling problem with linearized AC power flow equations, for large scale systems, does not tractable task without decomposition strategy. Accordingly, to solve proposed problem for large-scale systems, a Benders decomposition is applied to decompose the robust daily scheduling problem into a unit commitment and economic dispatch master problem and several linear AC grid constrained sub-problems. An adjustable linear AC robust daily scheduling model is developed to find a more robust solutions against uncertainties of WPG. Accordingly, to the best of authors' knowledge, the main contributions of this paper with respect to previous works in the area are as follows:

1) An adjustable robust min-max optimization framework is proposed for the linearized AC constrained daily scheduling problem (LAC-RDAS) with CPTs application. The proposed adjustable RA immunize the daily scheduling solution against different levels of uncertainties in WPG. To the best of our knowledge, there is no research work in the area which reports a linear robust AC daily scheduling model.

2) It is proved that the linear models of the TCT and PST improve the grid side flexibility with the linearized robust AC constrained daily scheduling in a coordinated framework to manage uncertain WPGs.

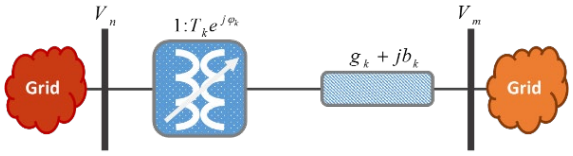

Fig. 1. A transmission line with tap changer and phase-shifting transformers.

3) In contrast to previous RA frameworks [11-15] which include DC model to find the worst case realizations, this paper considers a linearized AC model with linear models of CPTs model, which includes constraints pertaining to both voltage magnitude and reactive power.

2. Linearized models of TCT and PST in AC OPF

A linear approximation of AC power flow including TCT and PST is proposed in this section. The linearization is based on Taylor series expansion theory, binary expansion discretization approach, and piece wise linearization (PWL) and some innovative simple techniques described in [22]. The assumptions considered in the linearization process are: (i) The voltage magnitude of each bus is assumed to be around 1.0 per unit (p.u.), i.e., $0.95 \le V_n \le 1.05$, and (ii) the δ_k for line k is near to zero (or very small) which results $\sin(\delta_k) \approx \delta_k$ and $\cos(\delta_k) \approx 1$.It is to be noted that the models of the TCT and PST and fixed tap transformer are based on [3]. Fig. 1 shows the schematic of line n and m coupled with TCT/PST and the voltage/phase angle in line m is regulated by TCT/PST. The active and reactive power flows in the lines can be represented as follows,:

$$fl^P_{mn} = g_k\left(V_n^2 - T_k V_n V_m \cos\left(\delta_{mn} - \varphi_k\right)\right) + T_k V_n V_m b_k \sin(\delta_{mn} - \varphi_k) \quad (1)$$

$$fl^Q_{mn} = -b_k\left(V_n^2 - T_k V_n V_m \cos\left(\delta_{mn} - \varphi_k\right)\right) + T_k V_n V_m g_k \sin(\delta_{mn} - \varphi_k) \quad (2)$$

Where the sub-index k refers to the available component between buses n and m. and, T_k is the tap ratio of TCT k and φ_k is phase of the PST k.

Like voltage of buses, the tap position of tap changer is assumed to be around 1.0 per unit (p.u.), i.e., $0.95 \le T_k \le 1.05$, and by applying to the PWL approximation, (1) and (2) are linearized as follows:

$$fl^P_{nm} = g_k\left(V_n - V_m - T_k - \psi_{nm} + 2\right) - b_k\left(\delta_{mn} - \varphi_k\right) \quad (3)$$

$$fl^Q_{nm} = -b_k\left(V_n - V_m - T_k - \psi_{nm} + 2\right) - g_k\left(\delta_{mn} - \varphi_k\right) \quad (4)$$

Given the typical range of voltage angle with phase shifter angle is $\left|\delta_{mn} - \varphi_k\right| \le 10^\circ$, then the PWL approximation of, $\cos\left(\delta_{mn} - \varphi_k\right)$ is as follows:

$$\psi_{nm} = \alpha_{nm,\ell}\left(\delta_{mn} - \varphi_k\right) + \beta_{nm,\ell} \quad (5)$$

It is supposed that the transformer adjusts the voltage /phase at bus n, then, the active and reactive power flows can be represented as follows:

$$fl^P_{nm} = g_k\left(T_k^2 V_n^2 - T_k V_n V_m \cos(\delta_{nm} - \varphi_k)\right) + b_k T_k V_n V_m \sin(\delta_{nm} - \varphi_k) \quad (6)$$

$$fl^q_{nm} = -b_k\left(T_k^2 V_n^2 - T_k V_n V_m \cos(\delta_{nm} - \varphi_k)\right) - g_k T_k V_n V_m \sin(\delta_{nm} - \varphi_k) \quad (7)$$

The linear approximation of the equations (6) and (7) are as follows.

$$fl^P_{nm} = g_k\left(V_n + T_k - V_m - \psi_{nm}\right) - b_k\left(\delta_{mn} - \varphi_k\right) \quad (8)$$

$$fl^Q_{nm} = -b_k\left(V_n + T_k - V_m - \psi_{nm}\right) - g_k\left(\delta_{mn} - \varphi_k\right) \quad (9)$$

It is to be noted that in the equations (3) and(4)

(i) $k = (n,m) \in \Omega_{LTC}$, T_k is a decision variable and $\varphi_k = 0$

And in the equations (8) and (9)

(ii) $k = (n,m) \in \Omega_{PST}$, φ_k is a decision variable and T_k has a constant value;

For the other lines without TCT and PST

(iii) $k = (n,m) \in \Omega_k$, T_k is a constant value, i.e., $T_k = 1$ and $\varphi_k = 0$.

3. Problem formulation

3.1 Assumptions

For more clarifications, the assumptions of the proposed model are addressed below:

- Only WPG uncertainty is considered. However, the model is flexible to include other sources of the uncertainties for example: load uncertainty.

- The power factor of all wind farms is considered to be 1.

3.2 Deterministic daily scheduling formulation

The deterministic daily scheduling optimization problem has been extensively studied with MILP formulation [23, 24]. The objective function is to minimize the total operation costs, including thermal unit power generation cost including the startup and shutdown costs over the scheduling horizon. The mathematical formulation of the objective function is as follows:

$$Min \quad \sum_t \sum_g \left(C^b_g \cdot P^b_{gt} + C^{SU}_{gt} \cdot v_{g,t} + C^{SD}_{gt} \cdot w_{g,t}\right) \quad (10)$$

The constraints associated daily scheduling problem are system active load balance including power loss (11), capacity limits of active and reactive powers of thermal generating units (12)-(13), generation limits of WPG (13), startup and shutdown status of thermal units (15), the minimum up and down time (16) and (17), ramping up and down limits (18)-(19), the linear active and reactive transmission lines constraints (20)-(21), minimum and maximum limits for voltage magnitudes and bus angles (22)-(23), the lower and upper bounds for magnitude of tap changer and phase shifter angle by (24)-(25). The model also includes the linearized power flow equations of TCT and PST have been consederied in (26)-(28) similar constraints (2)-(3) and (8)-(9).

$$\sum_{g} P_{gt}^{b} + \sum_{w} P_{wt}^{b} = \sum_{n} D_{nt} + PL_{t} \tag{11}$$

$$u_{gt} \cdot P_{g,t}^{\min} \le P_{gt}^{b} \le u_{gt} \cdot P_{g,t}^{\max} \tag{12}$$

$$u_{gt} \cdot q_{g,t}^{\min} \le q_{gt}^{b} \le u_{gt} \cdot q_{g,t}^{\max} \tag{13}$$

$$0 \le P_{wt}^{b} \le P_{f,wt}^{b} \tag{14}$$

$$v_{g,t} - w_{g,t} = u_{g,t} - u_{g,t-1} \tag{15}$$

$$\sum_{t'=t-UT_g+1}^{t} v_{g,t'} \le u_{g,t}, \quad \forall g,t \in \left\{UT_g,...,T\right\} \tag{16}$$

$$\sum_{t'=t-DT_g+1}^{t} w_{g,t'} \le 1 - u_{g,t}, \quad \forall g,t \in \left\{DT_g,...,T\right\} \tag{17}$$

$$P_{g,t}^{b} - P_{g,t-1}^{b} \le R_g^{+} u_{g,t-1} + R_g^{SU} v_{gt} \tag{18}$$

$$P_{g,t-1}^{b} - P_{g,t}^{b} \le R_g^{+} u_{gt} + R_g^{SU} w_{gt} \tag{19}$$

$$P_{gt}^{b} + P_{wt}^{b} - \sum_{\forall k(m,n)} fl_{nmkt}^{P^u} = D_{nt} \tag{20}$$

$$q_{gt}^{b} - \sum_{\forall k(m,n)} fl_{nmkt}^{Q^u} = \gamma_{dt} \cdot Q_{nt} \tag{21}$$

$$V_n^{\min} \le V_{nt}^{b} \le V_n^{\max} \tag{22}$$

$$\delta^{\min} \le \delta_{nt}^{b} \le \delta^{\min} \tag{23}$$

$$\varphi_k^{\min} \le \varphi_k^{b} \le \varphi_k^{\max} \tag{24}$$

$$T_k^{\min} \le T_k^{b} \le T_k^{\max} \tag{25}$$

$$fl_{nmt}^{P^b} = g_k\left(V_{nt}^{b} - V_{mt}^{b} - T_{kt}^{b} - \psi_{nmt}^{b} + 2\right) - b_k\left(\delta_{nmt}^{b} - \varphi_{kt}^{b}\right) \tag{26}$$

$$fl_{nmt}^{Q^b} = -b_k\left(V_{nt}^{b} - V_{mt}^{b} - T_{kt}^{b} - \psi_{nmt}^{b} + 2\right) - g_k\left(\delta_{nmt}^{b} - \varphi_{kt}^{b}\right) \tag{27}$$

$$fl_{mnt}^{P^b} = g_k\left(V_{nt}^{b} + T_{kt}^{b} - V_{mt}^{b} - \psi_{mnt}^{b}\right) - b_k\left(\delta_{mnt}^{b} - \varphi_{kt}^{b}\right) \tag{28}$$

$$fl_{mnt}^{Q^b} = -b_k\left(V_{nt}^{b} + T_{kt}^{b} - V_{mt}^{b} - \psi_{mnt}^{b}\right) - g_k\left(\delta_{mnt}^{b} - \varphi_{kt}^{b}\right) \tag{29}$$

3.3 Robust daily scheduling formulation

Uncertainties associated with WPGs are characterized by means of polyhedral uncertainty sets as follows:

$$\Theta^{\Delta D_w} = \left\{ \begin{array}{l} P_{f,wt}^{b} - \tilde{P}_{wt} \le P_{wt}^{u} \le P_{f,wt}^{b} + \tilde{P}_{wt}, \\ \sum_{w}\sum_{t}\left|\frac{P_{wt}^{u} - P_{f,wt}^{b}}{\tilde{P}_{wt}}\right| \le \Delta D_w \end{array} \right\} \tag{30}$$

The size of $\Theta^{\Delta D_w}$ can be controlled with degree of robustness ΔD_w. The robust security constraints of the model are represented by set of equations from (31) to (44) to handle different uncertainty sources as defined by the uncertainty set (30). The uncertainty set includes wind energy forecast $P_{f,wt}^{b}$ with its forecast error $\tilde{P}_{wt}$ and budget levels of WPG uncertainty is ΔD_w. When $\Delta D_w = 0$, the uncertainty set will formulate a deterministic case. The increase in ΔD_w represents, wider range of deviations in the WPG forecasts. And the respective response to uncertainties in dispatches of thermal units, wind farm, bus voltage, angles, phase shifter angle, magnitude of tap changer, active and reactive power flow of lines in response are represented as follows, $\left\{P_{wt}^{u}\right\} \in U$, P_{gt}^{u}, P_{wt}^{u}, q_{gt}^{u}, $V_{n,t}^{u}$, $\delta_{n,t}^{u}$, φ_{kt}^{u}, T_{kt}^{u}, $fl_{nmkt}^{P^u}$ and $fl_{nmkt}^{q^u}$. The proposed model also includes robust AC security constraints in the set of equations from (31) to (44) for handling wind uncertainty as defined by the uncertainty set (30). Besides, constraint in (30) is used to control the level of robustness of the solution. Constraints (31) and (32) represents the nodal active and reactive power balance in response to uncertainties. Constraints (33) – (39) represents the response of equations (12)-(14) and (22)-(25) to wind uncertainty. Re-dispatch of thermal units dealing with wind uncertainty is limited by their corrective response rates and generation outputs in the base case (44).

$$P_{gt}^{u} + P_{wt}^{u} - \sum_{\forall k(m,n)} fl_{nmkt}^{P^u} = D_{nt} \tag{31}$$

$$q_{gt}^{u} - \sum_{\forall k(m,n)} fl_{nmkt}^{Q^u} = \gamma_{dt} \cdot Q_{nt} \tag{32}$$

$$0 \le P_{wt}^{u} \le P_{f,wt}^{b} \tag{33}$$

$$u_{gt} \cdot P_{g,t}^{\min} \le P_{gt}^{u} \le u_{gt} \cdot P_{g,t}^{\max} \tag{34}$$

$$u_{gt} \cdot q_{g,t}^{\min} \le q_{gt}^{u} \le u_{gt} \cdot q_{g,t}^{\max} \tag{35}$$

$$V_n^{\min} \le V_{nt}^{u} \le V_n^{\max} \tag{36}$$

$$\delta^{\min} \le \delta_{nt}^{u} \le \delta^{\max} \tag{37}$$

$$\varphi_k^{\min} \le \varphi_{kt}^{u} \le \varphi_k^{\max} \tag{38}$$

$$T_k^{\min} \le T_{kt}^{u} \le T_k^{\max} \tag{39}$$

$$fl_{nmt}^{P^u} = g_k\left(V_{nt}^{u} - V_{mt}^{u} - T_{kt}^{u} - \psi_{nmt}^{u} + 2\right) - b_k\left(\delta_{nmt}^{u} - \varphi_{kt}^{u}\right) \tag{40}$$

$$fl_{nmt}^{Q^u} = -b_k\left(V_{nt}^{u} - V_{mt}^{u} - T_{kt}^{u} - \psi_{nmt}^{u} + 2\right) - g_k\left(\delta_{nmt}^{u} - \varphi_{kt}^{u}\right) \tag{41}$$

$$fl_{mnt}^{P^u} = g_k\left(V_{nt}^{u} + T_{kt}^{u} - V_{mt}^{u} - \psi_{nmt}^{u}\right) - b_k\left(\delta_{nmt}^{u} - \varphi_{kt}^{u}\right) \tag{42}$$

$$fl_{mnt}^{Q^u} = -b_k\left(V_{nt}^{u} + T_{kt}^{u} - V_{mt}^{u} - \psi_{nmt}^{u}\right) - g_k\left(\delta_{nmt}^{u} - \varphi_{kt}^{u}\right) \tag{43}$$

$$\left|P_{gt}^{b} - P_{gt}^{u}\right| \le \Delta\Phi_g \tag{44}$$

4. Solution methodology

The suggested robust daily scheduling formulations in (10) – (44) is in the form of non-convex and nonlinear problem which in the case of large scale applications yields NP-hard problem. Therefore, Benders decomposition (BD) solution strategy is implemented to decompose the original problem into a master daily scheduling problem for the base case and tractable sub-problems for evaluating the base case with network-related constraints and the security check for WPG

uncertain interval. The detailed formulations for the master problem and each sub-problem, as well as the full algorithm steps are discussed in the following subsections.

4.1. Master daily scheduling problem

The master daily scheduling problem minimizes the base case operation cost, (10), subject to constraints (11) – (19) with all feasibility benders cuts discussed later.

4.2. Hourly grid security check for the base case

The hourly network evaluation sub-problem (45) checks the probable grid violations of the master scheduling results obtained from the base case as follows:

$$\Re_t = \sum_n (\Psi_{1,nt} + \Psi_{2,nt})$$

$$\hat{P}^b_{gt} + \hat{P}^b_{wt} - \sum_{\forall k(m,n)} fl^P_{nmkt} = D_{nt} + \Psi_{1,nt} - \Psi_{2,nt}$$

$$(20) - (26) \qquad (45)$$

$$P^b_{gt} = \hat{P}^b_{gt} \qquad : \xi^b_{gt} \quad \forall g,t$$

$$u_{gt} = \hat{u}_{gt} \qquad : \varsigma^b_{gt} \quad \forall g,t$$

where ξ^b_{gt} and ς^b_{gt} are dual variables corresponding to the P^b_{gt} and u_{gt} variables. If the objective value of (45) is larger than the pre-specified threshold, a feasibility cut (46) will be generated and added to the master problem.

$$\Re_t + \sum_g \xi^b_{gt}(P^b_{gt} - \hat{P}^b_{gt}) + \sum_g \varsigma_{gt}(u_{gt} - \hat{u}_{gt}) \le 0 \qquad (46)$$

4.3. Worst case realizations with the largest grid security violation

The largest minimum security violation when wind fluctuates within its bounded interval is specified by a max-min optimization problem (47) and (48) to compute the largest minimum violation.

$$\max_{\{P^u_{wt}\}} \min_{\{\Upsilon_{1,nt},\Upsilon_{2,nt},\Upsilon_{1,gt},P^u_{gt},P^u_{wt}\}} \sum_n (\Upsilon_{1,nt} + \Upsilon_{2,nt}) + \sum_g \Upsilon_{3,gt} \qquad (47)$$

$$P^u_{gt} + P^u_{wt} - \sum_{\forall k(m,n)} fl^P_{nmkt} = D_{nt} + \Upsilon_{1,nt} - \Upsilon_{2,nt} \quad \kappa_{1,nt}$$

$$q^u_{gt} - \sum_{\forall k(m,n)} fl^q_{nmkt} = \gamma_{nt} \cdot Q_{nt} \quad \kappa_{2,nt}$$

$$\hat{u}_{gt} \cdot P^{\min}_{g,t} \le P^u_{gt} \le \hat{u}_{gt} \cdot P^{\max}_{g,t} \quad \kappa_{3,gt}, \kappa_{4,gt}$$

$$\hat{u}_{gt} \cdot q^{\min}_{g,t} \le q^u_{gt} \le \hat{u}_{gt} \cdot q^{\max}_{g,t} \quad \kappa_{5,gt}, \kappa_{6,gt}$$

$$0 \le P^u_{wt} \le P^b_{f,wt} \quad \kappa_{7,wt}$$

$$V_n^{\min} \le V_{nt}^u \le V_n^{\max} \quad \kappa_{8,nt}, \kappa_{9,nt}$$

$$\delta^{\min} \le \delta^u_{nt} \le \delta^{\max} \quad \kappa_{10,nt}, \kappa_{11,nt}$$

$$\varphi^{\min}_k \le \varphi^u_{kt} \le \varphi^{\max}_k \quad \kappa_{12,kt}, \kappa_{13,kt}$$

$$T_k^{\min} \le T_{kt}^u \le T_k^{\max} \quad \kappa_{14,kt}, \kappa_{15,kt} \qquad (48)$$

$$-L^{\max}_k \le \overbrace{\left(g_k\left(V_{nt} + T_{kt} - V_{mt} - \psi_{nmt}\right) - b_k\left(\delta_{mnt} - \varphi_{kt}\right)\right)}^{fl^P_{nmkt}} \le L^{\max}_k$$

$\kappa_{16,kt}, \kappa_{17,kt}$

$$-\tilde{L}^{\max}_k \le \overbrace{\left(-b_k\left(V_{nt} + T_{kt} - V_{mt} - \psi_{nmt}\right) - g_k\left(\delta_{mnt} - \varphi_{kt}\right)\right)}^{fl^q_{nmkt}} \le \tilde{L}^{\max}_k$$

$\kappa_{18,kt}, \kappa_{19,kt}$

$$\left|P^u_{gt} - \hat{P}^b_{gt}\right| \le \Delta\Phi_g + \Upsilon_{3,gt} \quad \kappa_{20,gt}, \kappa_{21,gt}$$

$$\Theta^{\Delta D_w} = \left\{ \begin{array}{l} P^b_{f,wt} - \tilde{P}_{wt} \le P^u_{wt} \le P^b_{f,wt} + \tilde{P}_{wt}, \\ \sum_w \sum_t \left| \frac{P^u_{wt} - P^b_{f,wt}}{\tilde{P}_{wt}} \right| \le \Delta D_w \end{array} \right\}$$

To have better insight, the compressed matrix form of (49) is used to substitue the robust model (47) – (48). Where Υ_1, Υ_2 and Υ_3 represent vector of slack variables related to objective function (47). Also, $\{\kappa_{1,(\cdot)}, \kappa_{2,(\cdot)}, ..., \kappa_{21,(\cdot)}\}$ are corresponding dual variables of constraints (48).

$$\max_{\{P_{f,w}\}} \min_{\{\Upsilon_1,\Upsilon_2,\Upsilon_1,P,P_w\}} 1^T \cdot (\Upsilon_1 + \Upsilon_2 + \Upsilon_3) \qquad (49)$$

$$P + P_w - B \cdot fl^p - \Upsilon_1 + \Upsilon_2 = D \quad \kappa_1$$

$$q - B' \cdot fl^q = Q \quad \kappa_2$$

$$\hat{u} \cdot P^{\min} \le P \le \hat{u} \cdot P^{\max} \quad \kappa_3, \kappa_4$$

$$\hat{u} \cdot q^{\min} \le q \le \hat{u} \cdot q^{\max} \quad \kappa_5, \kappa_6$$

$$0 \le P_w \le P_{f,w} \quad \kappa_7$$

$$V^{\min} \le V \le V^{\max} \quad \kappa_8, \kappa_9$$

$$\delta^{\min} \le \delta \le \delta^{\max} \quad \kappa_{10}, \kappa_{11}$$

$$\varphi^{\min} \le \varphi \le \varphi^{\max} \quad \kappa_{12}, \kappa_{13} \qquad (50)$$

$$T^{\min} \le T \le T^{\max} \quad \kappa_{14}, \kappa_{15}$$

$$-L^{\max} \le \overbrace{\left(F \cdot V + G \cdot \delta + H \cdot T + K \cdot \varphi\right)}^{fl^p} \le L^{\max} \quad \kappa_{16}, \kappa_{17}$$

$$-L^{\max} \le \overbrace{\left(\tilde{F} \cdot V + \tilde{G} \cdot \delta + \tilde{H} \cdot T + \tilde{K} \cdot \varphi\right)}^{fl^q} \le L^{\max} \quad \kappa_{18}, \kappa_{19}$$

$$\left|P - \hat{P}\right| \le \Delta\Phi + \Upsilon_3 \Rightarrow \left\{ \begin{array}{ll} P - \Upsilon_3 \le \Delta\Phi + \hat{P} & \kappa_{20} \\ -P + \Upsilon_3 \le \Delta\Phi - \hat{P} & \kappa_{21} \end{array} \right.$$

and (30)

By applying the duality theory of the LP problem, the internal minimization problem represented by (49) and (50) can be converted into a maximization problem. Thus, (49) and (50) is reformulated by a single level linear optimization problem as shown in the equation (51). There are many methods to solve the linear optimization problem (51), such as branch and bound as explained in [11].

$$\max_{\{P_{f,w}\}} \begin{pmatrix} D\cdot\kappa_1 + Q\cdot\kappa_2 + P_{f,w}\cdot\kappa_3 + \hat{u}\cdot P^{\min}\cdot\kappa_4 + \hat{u}\cdot P^{\max}\cdot\kappa_5 \\ +\hat{u}\cdot q^{\min}\cdot\kappa_6 + \hat{u}\cdot q^{\max}\cdot\kappa_7 \\ +V^{\min}\cdot\kappa_8 + V^{\max}\cdot\kappa_9 + \delta^{\min}\cdot\kappa_{10} + \delta^{\max}\cdot\kappa_{11} + \varphi^{\min}\cdot\kappa_{12} \\ +\varphi^{\max}\cdot\kappa_{13} + T^{\min}\cdot\kappa_{14} + T^{\max}\cdot\kappa_{15} \\ +L^{\max}\cdot(\kappa_{17}-\kappa_{16}) + \tilde{L}^{\max}\cdot(\kappa_{19}-\kappa_{18}) \\ +(\Delta\Phi+\hat{P})\cdot\kappa_{20} + (\Delta\Phi-\hat{P})\cdot\kappa_{21} \end{pmatrix}$$

$$-1\le\kappa_1\le 1 \qquad -\kappa_{20}+\kappa_{21}\le 1$$

$$\kappa_1+\kappa_3-\kappa_4+\kappa_{20}-\kappa_{21}\le 0 \qquad (51)$$

$$\kappa_2+\kappa_5-\kappa_6\le 0 \qquad \kappa_1+\kappa_7\le 0$$

$$-(B\cdot F)^T\cdot\kappa_1-(B'\cdot\tilde{F})^T\cdot\kappa_2+\kappa_8-\kappa_9 + F^T\cdot(\kappa_{17}-\kappa_{16})+\tilde{F}^T\cdot(\kappa_{19}-\kappa_{18})\le 0$$

$$-(B\cdot G)^T\cdot\kappa_1-(B'\cdot\tilde{G})^T\cdot\kappa_2+\kappa_{10}-\kappa_{11} +G^T\cdot(\kappa_{17}-\kappa_{16})+\tilde{G}^T\cdot(\kappa_{19}-\kappa_{18})\le 0$$

$$-(B\cdot H)^T\cdot\kappa_1-(B'\cdot\tilde{H})^T\cdot\kappa_2+\kappa_{14}-\kappa_{15} +H^T\cdot(\kappa_{17}-\kappa_{16})+\tilde{H}^T\cdot(\kappa_{19}-\kappa_{18})\le 0$$

$$-(B\cdot K)^T\cdot\kappa_1-(B'\cdot\tilde{K})^T\cdot\kappa_2+\kappa_{12}-\kappa_{13} +K^T\cdot(\kappa_{17}-\kappa_{16})+\tilde{K}^T\cdot(\kappa_{19}-\kappa_{18})\le 0$$

and (30)

4.4 Worst case realizations with generation of feasibility benders cuts

If the highest minimum security violation obtained in (52) subject to constraints (53) is greater than the predefined threshold, the security checking sub-problem (52) – (53) will generate the feasibility Benders cut as per (54).

$$\min \Im = \sum_t\sum_n(\Upsilon_{1,nt}+\Upsilon_{2,nt})+\sum_g\Upsilon_{1,gt} \qquad (52)$$

Subject to:

$$P^b_{gt}(P^{worst}_{f,wt})+P_{wt}(P^{worst}_{f,wt}) - \sum_{\forall k(m,n)} fl^P_{nmkt}(P^{worst}_{f,wt}) = D_{nt}+\Upsilon_{1,nt}-\Upsilon_{2,nt}$$

$$(29)-(37) \text{ for } P^{worst}_{f,wt}$$

$$P^b_{gt}=\hat{P}^b_{gt} \qquad :\xi^u_{gt} \quad \forall g,t$$

$$u_{gt}=\hat{u}_{gt} \qquad :\varsigma^u_{gt} \quad \forall g,t \qquad (53)$$

$$\left|\hat{P}^b_{gt}-P_{gt}(P^{worst}_{f,wt})\right|\le\Delta\Phi_g+\Upsilon_{3,gt}$$

$$\hat{\Im}+\sum_t\sum_g\xi^u_{gt}(P^b_{gt}-\hat{P}^b_{gt})+\sum_t\sum_g\varsigma^u_{gt}(u_{gt}-\hat{u}_{gt})\le 0 \qquad (54)$$

Where ς^u_{gt} and ξ^u_{gt} are dual variables corresponding to P^b_{gt} and u_{gt} variables shown in (53). The Benders cut (54) is added to the master problem to get robust thermal unit scheduling solution results. The flowchart of proposed solution methodology is shown in Fig. 2. The proposed model consists the following steps:

Step I: In the base case (10), the master problem (MP) minimizes the operation cost subject to constraints (11) – (19) as well as generated Benders cuts later.

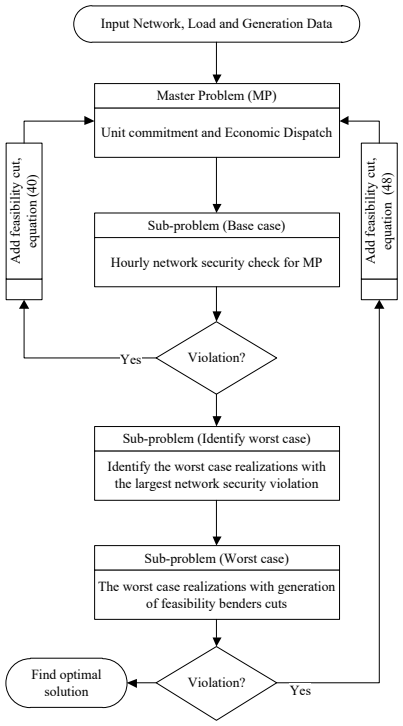

Fig. 2. Flowchart of the proposed solution methodology.

Step II: This step performs the hourly grid security check for MP optimal solutions, i.e., P^b_{gt} and u^b_{gt}. If the objective value (45) is larger than the prespecified threshold, the feasibility cut (46) will be generated and added to MP.

Step III: This step identifies the worst wind uncertainty realization P^{worst}_{wt} resulting in the largest minimum security violation, when WPG vary within its interval.

Step IV: In this step, if the largest minimum violation for the worst wind realization P^{worst}_{wt} is larger than the predefined threshold, the feasibility Benders cut (54) will be generated and fed back to MP for seeking robust thermal units commitment and economic dispatch solutions that would alleviate security violations.

The above iterative process stops when the master problem solution satisfies all security constraints, that is, there is no need to add more feasibility cuts in steps II and IV.

5 Case studies

In this section, the effectiveness and advantage of the proposed linear AC robust daily scheduling problem with TCT and PST is demonstrated by the six-bus system and modified IEEE 118-bus system. All case studies are executed using CPLEX 12.4 under GAMS software [25] on a PC with Intel Core i7, 4.5 GHz, processor and 16 GB memory.

5.1. The six–bus system

The six-bus system shown in Fig. 3 is used to illustrate the proposed linear AC robust daily scheduling problem, with co-operation of the TCT and PST devices. The system includes three thermal units, two transformers (i.e., the TCT and PST) one wind farm, and three loads. The characteristics of thermal units and transmission lines and TCT and PST are given in Tables 1-3. The respective corrective dispatch capabilities of the three thermal units are 9 MW, 8 MW, and 6 MW. The wind farm with a maximum power output of 200 MW is installed at bus 5. The wind farm with 200-MW capacity,

Table 1: Thermal units data and transmission line data; the 6-bus system.

Units	Energy bid price ($/MWh)	Start up/ Shut down cost ($)	P^{max} (MW)	P^{min} (MW)	Q^{max} (MVAr)	Q^{min} (MVAr)	Min Up (h)	Min Down (h)	Ramp up/down rate (MW/h)
G1	20	100/0	220	100	200	-80	4	4	55
G2	23	100/0	200	10	70	-40	3	2	50
G3	35	100/0	50	10	50	-40	1	1	20

Table 2: Transmission line data; the 6-bus system

Line no.	From Bus	To Bus	X(p.u.)	R(p.u.)	Max. line flow (MW)
1	1	2	0.17	0.005	50
3	2	3	0.037	0.022	150
4	2	4	0.197	0.007	150
5	3	6	0.018	0.005	150
6	4	5	0.037	0.002	50

Table 3: tap-changing transformer and phase shifter data; the 6-bus system

Line no.	TCT and PST	From Bus	To Bus	X(p.u.)	Max Tab/Angle	Min Tab/Angle	Max. line flow (MW)
2	TCT	1	4	0.037	0.95	1.05	150
7	PHT	5	6	0.018	25 (Deg)	-25 (Deg)	150

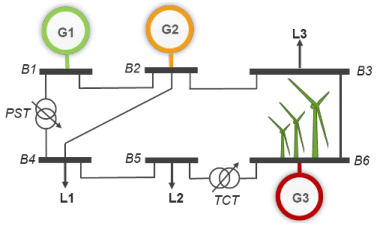

Fig. 3. One-line diagram of the six-bus system with TCT and PST and wind farm.

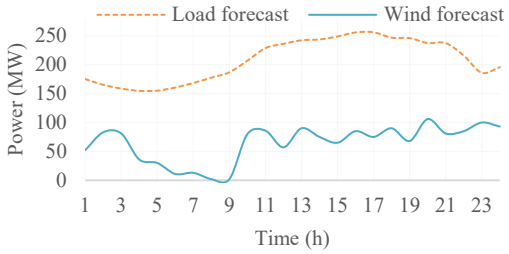

Fig. 4. Profiles of wind power and load forecasts.

consists of 134 Siemens 1.5 MW wind turbines spread over nearly 13,000 acres of land. The type of wind generators, in this paper, are the same as those located in the Northern flat lands of Texas [26]. Forecast values of the aggregated load and WPGs are shown in Fig. 4. Other system data can be found in [27]. Noted that, in this paper, the aim is not to propose a technique to determine the optimal location of TCT and PST (a method for optimal TCT and PST location can be found in [28]). The positions of TCT and PST have been selected based on the knowledge of the power grid and with the aim of improving the transmission congestion. The following four cases are considered to illustrate the performance of the proposed model with different levels of uncertainty set by the budget parameter.

Case 1) is base case without TCT and PST devices, and this case is considered as a reference case.

Case 2) studies the effect of TCT device in Case 1.

Case 3) studies the effect of the PST device in Case 1.

Case 4) studies the combined effect both TCT and PST devices in Case 1.

Case 1: In this case, the proposed LAC-RDAS problem, without TCT and PST model, is applied on the modified six-bus system. Fig.5 (a) shows operation costs with respect to different budget settings. The operation cost, in Case 1, increases as the degree of budget increases from zero to one. As the budget increases, more uncertainty is released and the optimization process has to provide a more robust solution to deal with the uncertainties. Therefore, the optimization process tries to use more reliable and expensive units in the operation to handle the uncertainties. Table 4 shows the three generator statuses for the period of 24 hours when the budget is 0. Similarly the Table 5 shows the status of the generators for the period of 24 hours when the budget is 1. It is evident from the Table 5, that the number of hours of service by the generator G3 is higher when the budget is 1 in comparison to the hours when the budget is 0 as shown in Table 4. The higher corrective capabilities to handle higher uncertainties were obtained by keeping the expensive thermal unit G3 inservice for more hours as shown in the Fig. 6. The corrective capacity of online regular thermal units is 40 MW when the budget is 0, while corrective capacity of thermal units (CCOTU) is 553.1 MW when the budget is 1. Also, the power flow lines 1–2 and 4–5 has exceeded their capacity as they have lower capacities compared to other lines. Therefore, the expensive unit G3 is kept in service to mitigate violations. For example, the lines 1-2 and 4–5 are congested at hours 7–12 which leads to not commitment of unit G1 and the residual load is supported by expensive G3. The other main reason for increase in operating cost is system voltage magnitude. As shown in Fig. 6 (a) and (b), for Case 1, when budget setting is changed from 0 to 1, the voltage magnitude (VM) at the most buses are decreasing which create a new critical issue in system operation and caused to increase operation cost. To overcome this issue, additional commitment of new (expensive) unit, i.e., unit G3 in this case, is needed to increase reactive power generation and inject to buses to improve voltage magnitude and lead to a higher stochastic operation cost.

Case 2: In this case, a TCT is introduced in the line 5-6. The operational cost for the case 2 is shown in Figs. 5-7. The operational status of the generators when the budget is 0 and 1 are given in the Tables 4 and 5 respectively. As mentioned in previous case, drop in buses voltage magnitude is one of reasons for the increased operation cost. In the absence of TCT, the reactive power generated by the thermal units would overcome this voltage problem partially with additional operation cost. As shown in Fig.6. (a) and (b), the TCT device is able to significantly improve voltage magnitude at most buses and overcome this issue by adjusting transformer tap. For instance, in Case 1 when the budget is 0, the voltage magnitude at bus 6 in hours 13–14 is low.

Table 4: Hourly commitment status of units in Case 1-4; for budget $\frac{\Delta D_w}{NT} = 0$.

Cases	Units	24-Hours																							
Case 1	G1	1	0	0	0	0	0	0	0	0	0	0	1	1	1	1	1	1	1	1	1	1	1	0	0
	G2	1	1	1	1	1	1	1	1	1	1	1	1	1	1	1	1	1	1	1	1	1	1	1	1
	G3	0	1	0	0	0	0	1	1	1	1	1	1	1	1	0	0	0	0	0	0	0	0	1	0
Case 2	G1	1	0	0	0	0	0	0	0	0	0	0	1	1	1	1	1	1	1	1	1	1	1	0	0
	G2	1	1	1	1	1	1	1	1	1	1	1	1	1	1	1	1	1	1	1	1	1	1	1	1
	G3	0	1	0	0	0	0	1	1	1	1	1	1	0	0	0	0	0	0	0	0	0	0	1	0
Case 3	G1	0	0	0	1	1	1	1	1	1	1	1	1	1	1	1	1	1	1	1	1	1	1	0	0
	G2	1	1	1	1	1	1	1	1	1	1	1	1	1	1	1	1	1	1	1	1	1	1	1	1
	G3	1	0	1	0	0	1	1	1	1	1	0	1	0	1	1	1	1	1	1	0	0	0	1	1
Case 4	G1	0	0	0	1	1	1	1	1	1	1	1	1	1	1	1	1	1	1	1	1	1	1	0	0
	G2	1	1	1	1	1	1	1	1	1	1	0	0	0	0	0	0	0	0	0	0	1	1	1	1
	G3	0	0	1	0	0	0	0	1	1	0	0	0	0	0	0	0	0	0	0	0	0	0	1	0

Table 5: Hourly commitment status of units in Case 1-4; for budget $\frac{\Delta D_w}{NT} = 1$.

Cases	Units	24-Hours																							
Case 1	G1	0	0	0	0	0	0	0	0	0	0	0	1	1	1	1	1	1	1	1	1	1	1	0	0
	G2	1	1	1	1	1	1	1	1	1	1	1	1	1	1	1	1	1	1	1	1	1	1	1	1
	G3	1	1	1	1	1	1	1	1	1	1	1	1	1	1	1	1	1	1	1	1	1	1	1	1
Case 2	G1	1	0	0	0	0	0	0	0	0	0	0	1	1	1	1	1	1	1	1	1	1	1	0	0
	G2	1	1	1	1	1	1	1	1	1	1	1	1	1	1	1	1	1	1	1	1	1	1	1	1
	G3	1	1	1	1	1	1	1	1	1	1	1	1	1	1	1	1	1	1	1	1	1	1	1	1
Case 3	G1	0	0	0	1	1	1	1	1	1	1	1	1	1	1	1	1	1	1	1	1	1	1	0	0
	G2	1	1	1	1	1	1	1	1	1	1	1	1	1	1	1	1	1	1	1	1	1	1	1	1
	G3	1	1	1	0	1	1	1	1	1	1	1	1	1	1	1	1	1	1	1	1	1	1	1	1
Case 4	G1	0	0	0	1	1	1	1	1	1	1	1	1	1	1	1	1	1	1	1	1	1	1	0	0
	G2	1	1	1	1	1	1	1	1	1	1	1	1	1	1	1	1	1	1	1	1	1	1	1	1
	G3	1	1	1	0	1	0	0	1	1	1	1	1	1	1	1	1	1	1	1	1	1	1	1	1

This is compensated by additional reactive power injection at this bus, by the expensive thermal unit G3 which is turned on at hours 13–14 (as shown in Table 5). The total number of hours of operation of G3 is 2 hours less for case 2 in comparison to case 1 when the budget is 0, which reduces the operational cost for case 2 The voltage and line limits contribute to lower 1.9% of the operation cost. The binding constraints provide restrictions on lines and voltage limits (in particular, at bus 6). As TCT is effectively voltage control device, it mitigates the voltage issues. Otherwise, as shown in Tables 4 and 5, the new unit commitment is mostly same as the schedule in Case 1. Therefore, the corrective capacities of thermal units increases slightly with the increase uncertainty budget level when compared to the previous case.

Case 3: In this case, in comparison to case 1, a PST is introduced in line 1-4. As mentioned in Case 2, the security constraints that limits power flow through lines and bus voltage (in particular, on line 4–5 and at bus 6) which causes lower 1.9% operation cost reduction,. As shown in Fig.5 (a) and 7, the TCT device by controlling voltage levels can reduce the cost or improve the system robustness. Nevertheless, the effects of this device on power flow through transmission lines are negligible, as this device controls only voltage levels. However, the voltage control can not improve the cost reduction beyond 1.9 % and it is associated with the constraints that limits the power flow through lines (in particular, through line 4–5). As shown in Fig.5 (a), the PST is most effective device for operational cost reduction in comparison with TCT, as PST can control the power flow. In Case 1, when budget is 0, due to the congestion in line 1-4 and 4-5, the cheapest unit G1 can be utilized only for 12 hours. Also the shortfalls in the wind generation is compensated by the expensive thermal unit G3 instead of G1. Therefore, a lower utilization of unit G1 that leads to a higher operating cost. The PST application in this case, mitigate the congestion in lines 1-2 and 2-4, and increase the commitment of G1 by 8 hours. Therefore, the overall operational cost is reduced drastically in comparison to case 1, even if the uncertainty budget is increased from 0 to 1 as shown in Fig. 5 (a) and (b) Also, the PST device improves the corrective capacities of online regular thermal units significantly and reduce the operational cost when compared with the case 2. Therefore, the PST device is more effective than the TCT device to enhance the system capacity and robustness.

Case 4: In the previous cases 2 and 3, the effect of TCT and PST were studied separately. Case 4 illustrates their combined effect. The combined effect of TCT and PST will bring both voltage and power flow control and can lead to comparatively cheaper solution whole range of uncertainty budget. In this case, the shortcomings of Case 3 is resolved by employing TCT device and the results are shown in Fig. 5, Table 4 and 5. Also, for calculating the contribution of TCT and PST in this test system, at first, the operation costs for different budget rate in Case 1 are taken as the baseline for the comparisons. Accordingly, the contribution of the TCT and PST in the proposed model for different budget rates have different values but this difference is very low. For example, as can be seen in Fig. 5 (a), for 0.2 budget rate, the contributions of TCT, PST, and both CPTs to the operation cost reduction are 1.5% (Case 2), 18% (Case 3) and 23.5% (Case 4) respectively.

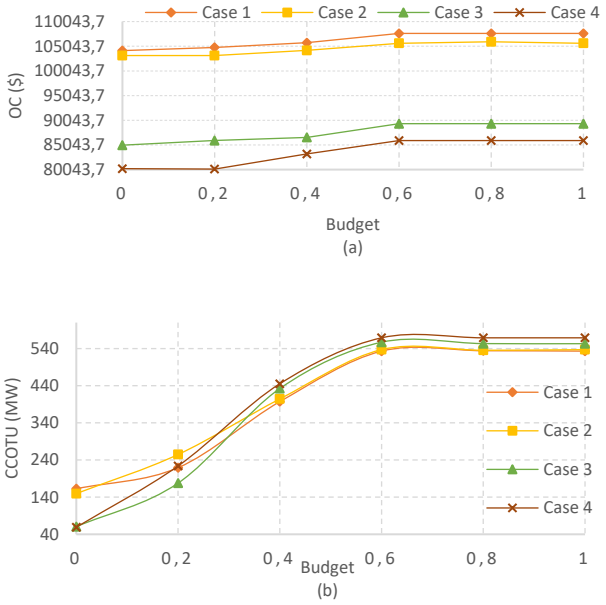

Fig.5. (a) Operation costs (OC) and (b) corrective capacities of thermal units (CCOTU) in different budget $\frac{\Delta D_w}{NT}$.

Similarly, for budget rate equal to 1, these contributions are 1.8% (Case 2), 17% (Case 3) and 21% (Case 4).

In the Fig. 6, the top plot shows the voltage levels on each buses for all cases, when the uncertainty budget is 0. Similarly the bottom plot shows the voltage levels in each buses for all cases when the uncertainty budget is 1. It is explicitly visible from Fig. 6, that the TCT device improves the voltage in bus 6 which reduces the commitment of the expensive thermal unit G3 and increases the commitment of inexpensive thermal unit G1. On other hand, the PST device improves the congestion control by independent control of voltage angle at buses 1 and 4 and increase the commitment of inexpensive unit G1 (as shown in Table 4). Finally, in the case of concurrent operation of the TCT and PST devices, the operation cost for all of budget levels is decreased significantly while corrective capacities of online thermal units are increased in comparison to using these devices independently. This is well expected because, two major challenges are existing in the proposed problem, the first is the transmission congestion, and the second is the wind uncertainty, so, when the budget rate is equal to zero the wind uncertainty does not exist in the system. In this condition, the congestion plays important role in the system. Accordingly, the transmission congestion in the power grid can be effectively removed by the CPTs and lead to lower committed expensive units. In this test system, the congestion at peak hours can be mitigated by the committed unit G3 and the wind uncertainty can be covered by committing the unit G2 and it doesn't need to commit the unit G3 for all hours. For example, for zero budget rate, the relatively cheaper unit G2 is on at all hours while the G3 is used at the peak hours to mitigate the congestion and minimize the total operation cost (this fact has been shown in Table 5). But, when the budget rate is equal to 1, both wind uncertainty and transmission congestion are existed in the system, but, in such situations, the wind uncertainty problem is more serious than the congestion problem in the system that it can be mitigated by more allocating corrective capacities with more committed units with aim to cover uncertainty.

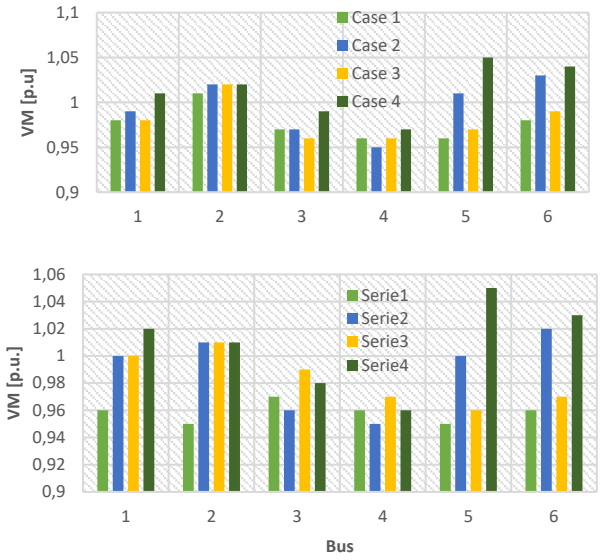

Fig.6. (a) voltage magnitude (VM) for $\frac{\Delta D_w}{NT}=0$ and (b) for $\frac{\Delta D_w}{NT}=1$.

Fig. 7. The number of committed units in different budget $\frac{\Delta D_w}{NT}$.

Also, when the uncertainty in the system is high, the influence of CPTs on the operation cost reduction is low. Accordingly, with increasing the budget rate, the operation cost saving is decreased incrementally. For example, since the wind farm is installed in the bus 6, with more WPGs, the power through the lines connected to bus 6 are increased. In this condition, power flowing through lines 3-6 and 5-6 will violate the their ratings. Therefore, the expensive G3 is committed to help alleviating these violations. On the other hand, for the budget rate more than 0.6, the wind uncertainty is high, and also the wind uncertainty is in the critical level at most hours; in a such situation, the wind uncertainty is covered by unit G3, for this reason, this unit is on at all hours (as shown in Table 5). Similarly, when the budget rate is more than 0.6, units G2 and G3 are committed for all hours, and number of committed units is in its highest values for all cases. For example, as can be seen in Fig.7, with a smaller uncertainty range, i.e., the budget rate less than 0.6, fewer units are committed for the all cases. Thus, for the budget rate more than 0.6, the number of committed units has the highest values and the corrective capacity of thermal units reaches its capacity limit for all cases. So, based on these facts, the operation cost and corrective capacities of units reach their own highest value and, these values are not more increased for the budget rate more than 0.6.

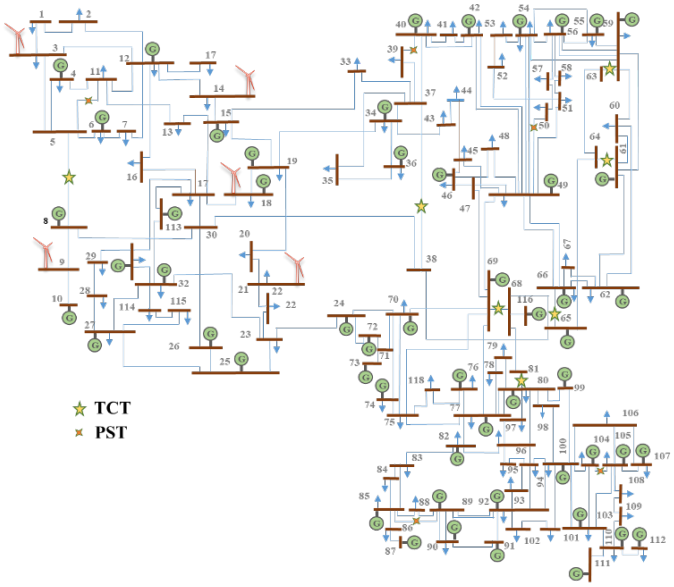

Fig. 8. The Modified IEEE 118-bus system.

5.2. The modified IEEE 118-bus system

The modified IEEE 118-bus system is used to illustrate the effectiveness of the suggested adjustable LAC-RDAS problem for the larger system. A can be seen in Fig.8, the system consists of 54 thermal units, 5 wind farms, 186 branches and 91 loads. The hourly active and reactive loads as well as the characteristics of units and lines are taken from http://motor.ece.iit.edu/data. Additionally, five 200-MW wind farms are attached to buses 3, 9, 14, 18, and 22. Accordingly, the degree of robustness have the integer values between 0 and 5 (i.e., $0 \le \frac{\Delta D_w}{NT} \le 5$). Based on load flow analysis, the heavily loaded lines with low capacity in the modified IEEE 118–bus system are lines [11 (bus 5–bus 11), 55 (bus 39–bus 40), 70 (bus 49–bus 50), 136 (bus 85–bus 89) and 168 (bus 104–bus 105)] where the TCT devices are located. Similarly, for lines 5–8, 37–38, 59–63, 61–64, 65–66, 68–69 and 80–81, the PST devices are located. Four cases as described in the previous section were studied. Also, for this test system, an additional case (Case 5) has been studied to compare the proposed RA and the other RA in [11], for handling wind uncertainty.

The proposed linear AC robust optimization for large-scale test system is an NP-hard problem with the ac-grid constraints will dramatically increase the computation burden. Therefore, the benders decomposition technique is applied to solve proposed problem for this test system, the solution time needed to solve proposed problem, for each uncertainty budget level, is less than 25 min, which is reasonable for this test system. Table 6 shows the operation cost, and corrective capacities of online regular thermal units for different uncertainty budgets, for different cases from 1 to 4. The results for the 118 bus system are consistent with the results of 6-bus system. The results are given in Table 6 Similar to the 6-bus system, in the 118-bus system, for case 1 the voltage magnitude issues are partially overcome by increading the commitment of expensive thermal units, which increases the operational cost. As shown in case 3, the transmission congestion plays major role for opertational cost reduction beyond 0.7 %.

Table 6: Comparison of results for different cases in the 118-bus system

Cases	IEEE-118 bus	$\frac{\Delta D_w}{NT}=0$	$\frac{\Delta D_w}{NT}=2.5$	$\frac{\Delta D_w}{NT}=5$
Case 1	OC (M$)	1.134	1.173	1.192
	CCTU (MW)	720	2130	3769
Case 2	OC (M$)	1.126	1.169	1.188
	CCTU (MW)	820	2241	3834
Case 3	OC(M$)	1.114	1.162	1.175
	CCTU (MW)	890	2367	3956
Case 4	OC (M$)	1.105	1.156	1.168
	CCTU (MW)	920	2413	4132

Table 7: Results of RA in [11] for different cases in the 118-bus system

Cases	IEEE-118 bus	$\frac{\Delta D_w}{NT}=0$	$\frac{\Delta D_w}{NT}=2.5$	$\frac{\Delta D_w}{NT}=5$
Case 1	OC (M$)	1.134	1.179	1.201
	CCOTU (MW)	720	2340	3876
Case 2	OC (M$)	1.126	1.177	1.193
	CCOTU (MW)	820	2453	3987
Case 3	OC(M$)	1.114	1.171	1.183
	CCOTU (MW)	890	2563	4154
Case 4	OC (M$)	1.105	1.165	1.177
	CCOTU (MW)	920	2654	4342

The results indicates the PST device plays an important role in operational cost reduction by managing the congestion in the transmission lines which has lower limits similar to the previous 6-bus system. Thus the operation cost and corrective capacities of online regular thermal units have the lowest and highest values for Case 4 and 1 respectively.

Finally, the combined effect of TCT and PST devices, have the highest robustness and lowest operation cost for a large-scale system. In the Case 5, the proposed RA and the other RA in [11], for handling the wind uncertainty in the proposed LAC-RDAS problem, are compared in two aspects: (i) the operation cost (OC); (ii) the corrective capacities of thermal units (CCOTUs). The performance of the two approaches under different wind uncertainty budget levels are also investigated. Table 7 reports the OC and CCOTUs of the proposed RA and the RA in [11] with respect to the different wind uncertainty budget levels. As can be seen in this table, once the budget level increases, the OCs and CCOTUs of both approaches are increasing because more thermal units need to be committed to cover a wider range of the wind uncertainties. Once the budget level is 0, the OCs and CCOTUs of the both methods are the same as $1,116,970.07 and 213 MW, respectively. With the budget level larger than zero, the RA in [11] has relatively higher OCs and CCOTUs than the proposed model. Differences in the OCs and CCOTUs are mainly caused by the ways of how these two RAs handle uncertainties. In the proposed RA, the system is considered to be operated under the base case with unit dispatch and commitment decisions corresponding to the forecasted values and in the day-ahead scheduling, and

thermal units output will be securely and adaptively adjusted based on the corrective capabilities of thermal units once possible realizations of the wind uncertainties occur in the real time. For the RA in [11], the system is intended to be operated only with the UC decisions corresponding to the worst case uncertainty in the day-ahead scheduling problem, and thermal units output are adaptively determined based on the robust UC decisions once the possible realizations of the wind uncertainties occur. The basic idea is that if a UC solution could manage the worst case uncertainty, it could be able to find a secure dispatch solution for managing any uncertainty. In summary, the savings in the OCs is caused by the robust thermal unit dispatch and commitment solutions corresponding to the base case and the corrective capabilities of thermal units in the proposed model as compared to the RA solutions corresponding to the worst case uncertainty in [11]. Finally, the LAC-RDAS problem with our proposed RA could provide more economical and reliable dispatch information for day ahead and real-time markets.

6. Conclusion

Due to the impacts of high penetration wind energy and associated uncertainty factors, the secure and economic operation of power systems become critical. This paper proposes an adjustable robust daily scheduling model, based on grid ac-constraints, for a transmission system in the presence of TCT and PST devices and uncertain wind generation. The proposed robust optimization with the TCT and PST devices is an MINLP problem that is transformed into an MILP by the proposed method. The transformed linear AC robust optimization problem with linear TCT and PST device models can be solved by available efficient commercial grade software. In addition, the proposed robust optimization solution is protected against any occasion of uncertain WPGs within the uncertainty set. This paper points out that the operation cost increases as the degree of robustness or the budget level increases. The effect of the TCT and PST devices on the unit commitment, operation cost, and corrective capacity procedure is simulated and discussed in detail using the modified six-bus and IEEE 118-bus system (as a real-size model). Also, according to the case studies, the obtained results have a similar behavior. The simulation results approve the well-functioning of the application of these devices to decrease operation cost and increase robustness solution. Finally, the simulation results show that the lowest operation cost in the highest system's level of robustness (or highest budget) would be acquired by coordination of these devices in the proposed framework.

7 References

[1] M. Alizadeh, M. P. Moghaddam, N. Amjady, P. Siano, and M. Sheikh-El-Eslami, "Flexibility in future power systems with high renewable penetration: A review," *Renewable and Sustainable Energy Reviews,* vol. 57, pp. 1186-1193, 2016.

[2] P. G. Thakurta, R. Belmans, and D. Van Hertem, "Risk-based management of overloads caused by power injection uncertainties using power flow controlling devices," *IEEE Transactions on Power Systems,* vol. 30, no. 6, pp. 3082-3092, 2015.

[3] R. Zarate-Minano, A. Conejo, and F. Milano, "OPF-based security redispatching including FACTS devices," *IET generation, transmission & distribution,* vol. 2, no. 6, pp. 821-833, 2008.

[4] K. Imhof, F. Oesch, and I. Nordanlycke, "Modelling of tap-changer transformers in an energy management system," in *Power Industry Computer Application Conference, 1995. Conference Proceedings., 1995 IEEE*, 1995, pp. 378-384: IEEE.

[5] H. Ohtsuki, A. Yokoyama, and Y. Sekine, "Reverse action of on-load tap changer in association with voltage collapse," *IEEE Transactions on Power Systems,* vol. 6, no. 1, pp. 300-306, 1991.

[6] T. Ding, R. Bo, Z. Bie, and X. Wang, "Optimal selection of phase shifting transformer adjustment in optimal power flow," *IEEE Trans. Power Syst,* vol. 32, no. 3, pp. 2464-2465, 2017.

[7] A. Marinakis, M. Glavic, and T. Van Cutsem, "Minimal reduction of unscheduled flows for security restoration: Application to phase shifter control," *IEEE Transactions on Power Systems,* vol. 25, no. 1, pp. 506-515, 2010.

[8] D. O. Sidea, L. Toma, and M. Eremia, "Sizing a phase shifting transformer for congestion management in high wind generation areas," in *PowerTech, 2017 IEEE Manchester*, 2017, pp. 1-6: IEEE.

[9] M. Aien, A. Hajebrahimi, and M. Fotuhi-Firuzabad, "A comprehensive review on uncertainty modeling techniques in power system studies," *Renewable and Sustainable Energy Reviews,* vol. 57, pp. 1077-1089, 2016.

[10] J. Aghaei, A. Nikoobakht, P. Siano, M. Nayeripour, A. Heidari, and M. Mardaneh, "Exploring the reliability effects on the short term AC security-constrained unit commitment: A stochastic evaluation," *Energy,* vol. 114, pp. 1016-1032, 2016.

[11] D. Bertsimas, E. Litvinov, X. A. Sun, J. Zhao, and T. Zheng, "Adaptive robust optimization for the security constrained unit commitment problem," *IEEE Transactions on Power Systems,* vol. 28, no. 1, pp. 52-63, 2013.

[12] B. Hu and L. Wu, "Robust SCUC considering continuous/discrete uncertainties and quick-start units: A two-stage robust optimization with mixed-integer recourse," *IEEE Transactions on Power Systems,* vol. 31, no. 2, pp. 1407-1419, 2016.

[13] C. Dai, L. Wu, and H. Wu, "A multi-band uncertainty set based robust SCUC with spatial and temporal budget constraints," *IEEE Transactions on Power Systems,* vol. 31, no. 6, pp. 4988-5000, 2016.

[14] E. Heydarian-Forushani, M. Golshan, M. Moghaddam, M. Shafie-Khah, and J. Catalão, "Robust scheduling of variable wind generation by coordination of bulk energy storages and demand response," *Energy Conversion and Management,* vol. 106, pp. 941-950, 2015.

[15] A. Nikoobakht and J. Aghaei, "IGDT-based robust optimal utilisation of wind power generation using coordinated flexibility resources," *IET Renewable Power Generation,* vol. 11, no. 2, pp. 264-277, 2016.

[16] M. R. Bussieck and A. Drud, "SBB: A new solver for mixed integer nonlinear programming," *Talk, OR,* 2001.

[17] H. Ambriz-Perez, E. Acha, and C. Fuerte-Esquivel, "Advanced SVC models for Newton-Raphson load flow and Newton optimal power flow studies," *IEEE transactions on power systems,* vol. 15, no. 1, pp. 129-136, 2000.

[18] T. Nireekshana, G. K. Rao, and S. S. N. Raju, "Enhancement of ATC with FACTS devices using real-code genetic algorithm," *International Journal of Electrical Power & Energy Systems,* vol. 43, no. 1, pp. 1276-1284, 2012.

[19] P. Belotti, "Couenne: a user's manual," Technical report, Lehigh University2009.

[20] A. S. Drud, "CONOPT—a large-scale GRG code," *ORSA Journal on computing,* vol. 6, no. 2, pp. 207-216, 1994.

[21] A. Nikoobakht, J. Aghaei, M. Parvania, and M. Sahraei-Ardakani, "Contribution of FACTS devices in power systems security using MILP-based OPF," *IET Generation, Transmission & Distribution,* 2018.

[22] T. Akbari and M. T. Bina, "Linear approximated formulation of AC optimal power flow using binary discretisation," *IET Generation, Transmission & Distribution,* vol. 10, no. 5, pp. 1117-1123, 2016.

[23] A. Nikoobakht, J. Aghaei, and M. Mardaneh, "Managing the risk of uncertain wind power generation in flexible power systems using information gap decision theory," *Energy,* vol. 114, pp. 846-861, 2016.

[24] A. Nikoobakht and J. Aghaei, "IGDT-Based Robust Optimal Utilization of Wind Power Generation Using Coordinated Flexibility Resources," *IET Renewable Power Generation,* 2016.

[25] GAMS. The Solver Manuals. 1996 [Online]. Available: http://www.gams.com/.

[26] Alliance for Sustainable Energy, Department of Energy (DOE), Nat. Renew. Renewable Energy Lab. (NREL), System Advisor Model version 2014.1.14.

[27] A. Nikoobakht, M. Mardaneh, J. Aghaei, V. Guerrero-Mestre, and J. Contreras, "Flexible power system operation accommodating uncertain wind power generation using transmission topology control: an improved linearised AC SCUC model," *IET Generation, Transmission & Distribution,* vol. 11, no. 1, pp. 142-153, 2017.

[28] J. Peschon, D. S. Piercy, W. F. Tinney, and O. J. Tveit, "Sensitivity in power systems," *IEEE Transactions on Power Apparatus and Systems,* no. 8, pp. 1687-1696, 1968.